The equation of state of isotropic fluids of hard convex bodies from a high-level virial expansion

X.-M. You
Department of Chemistry, University of Manchester, Manchester M13 9PL, United Kingdom

A. Yu. Vlasov
Department of Chemistry, St. Petersburg State University, 26 Universitetsky Pr., 198504, St. Petersburg, Russia

A. J. Masters[a)]
Department of Chemistry, University of Manchester, Manchester M13 9PL, United Kingdom

(Received 6 May 2005; accepted 9 June 2005; published online 28 July 2005)

We have calculated virial coefficients up to seventh order for the isotropic phases of a variety of fluids composed of hard aspherical particles. The models studied were hard spheroids, hard spherocylinders, and truncated hard spheres, and results are obtained for a variety of length-to-width ratios. We compare the predicted virial equations of state with those determined by simulation. We also use our data to calculate the coefficients of the *y* expansion [B. Barboy and W. M. Gelbart, J. Chem. Phys. **71**, 3053 (1979)] and to study its convergence properties. Finally, we use our data to estimate the radius of convergence of the virial series for these aspherical particles. For fairly spherical particles, we estimate the radius of convergence to be similar to that of the density of closest packing. For more anisotropic particles, however, the radius of convergence decreases with increased anisotropy and is considerably less than the close-packed density. © *2005 American Institute of Physics*. [DOI: 10.1063/1.1992471]

I. INTRODUCTION

The virial equation of state (EOS) has a very sound theoretical foundation. Each virial coefficient is given by an exact expression involving the potential of interaction,[1–3] and so this approach is free from any *ad hoc* assumptions such as those that often appear in integral equation theory, perturbation theory, and other liquid-state methodologies.[3] Provided the series converges, one may systematically improve one's predictions by adding more terms in the series. Unfortunately little is known about the radius of convergence of the series. There exist rigorous results that give a lower bound for the radius of convergence[4,5] but, for hard-disc and hard-sphere fluids at least, it is clear that this lower bound lies considerably below the true value.[6–15] In order to get better estimates, one must resort to numerical work—i.e., to calculate as many virials as possible and try to numerically analyze the behavior of the series. The first ten virial coefficients have been calculated for hard discs and hard spheres[6–13] and the indications are that the radius of convergence is close to the density of closest packing.[9,14,15]

It is interesting to ask whether this might be a general result for all hard bodies—i.e., that the virial series converges for all densities less than that of close packing. Unfortunately for systems of aspherical particles, such as spheroids, spherocylinders, and truncated spheres, the virials have only been calculated up to fifth order.[13,16–21] One needs more data than this in order to do reasonable numerical work. In this article we present our results for the sixth and seventh virials for these systems so that we are in a better position to analyze the behavior of the series. We have also calculated the eighth virial, but we prefer to present these data in a later publication when we have reduced the associated statistical errors.

Apart from trying to contribute to the discussion on the radius of convergence, we hope our calculations will be useful in other ways. Firstly, a knowledge of the virial coefficients can help fix the values of otherwise unknown parameters that appear in approximate equations of state or, alternatively, can act as a check as to the quality of such approximate expressions. Good equations of state for reference fluids are an essential prerequisite for calculations on real fluids using perturbation theory. Secondly, sufficiently aspherical hard convex body models can form liquid-crystalline phases and it would be nice if one could calculate the phase behavior of such systems theoretically. To date, most such theories use approximate approaches based on the knowledge of the orientationally dependent second virial coefficient,[22–25] though we note some examples in which the effects of the third virial were also included.[26–28] In future papers we will present such an analysis, using higher-order virials to calculate the phase diagram.

The plan of this article is as follows. In Sec. II we present our results for high-order virial coefficients for hard spheroids, hard spherocylinders, and truncated hard spheres of a variety of length-to-width ratios and we discuss the trends that are found. In Sec. III we use the data to calculate equations of state and we compare these with simulation results, drawing qualitative conclusions about the conver-

[a)]Author to whom correspondence should be addressed. FAX: +161 275 4734. Electronic mail: Andrew.Masters@man.ac.uk

TABLE I. The reduced virial coefficients ($\tilde{B}_3$ to $\tilde{B}_7$) for hard spheroids (semimajor axis a and semiminor axis b) and the second virial B_2 in terms of the spheroid volume v_0. The estimated error is the final figure given in parentheses.

a/b	$B_2/(4v_0)$	$\tilde{B}_3$	$\tilde{B}_4$	$\tilde{B}_5$	$\tilde{B}_6$	$\tilde{B}_7$
1/10	3.2978	0.485 40(2)	$7.782(2)\times10^{-2}$	$-3.158(3)\times10^{-2}$	$-1.674(6)\times10^{-2}$	$-1.77(7)\times10^{-3}$
10	3.2978	0.314 30(2)	$-1.888(2)\times10^{-2}$	$2.140(3)\times10^{-2}$	$-2.25(7)\times10^{-3}$	$-7.0(1)\times10^{-3}$
1/7	2.4434	0.502 35(2)	0.102 87(2)	$-1.661(9)\times10^{-2}$	$-1.282(1)\times10^{-2}$	$-2.08(6)\times10^{-3}$
7	2.4434	0.379 50(2)	$2.049(2)\times10^{-2}$	$1.155(8)\times10^{-2}$	$5.87(4)\times10^{-3}$	$-6.81(1)\times10^{-3}$
1/5	1.8880	0.523 22(2)	0.134 26(2)	$3.26(3)\times10^{-3}$	$-6.96(6)\times10^{-3}$	$-1.14(6)\times10^{-3}$
5	1.8880	0.442 83(2)	$7.233(2)\times10^{-2}$	$1.227(3)\times10^{-2}$	$8.03(6)\times10^{-3}$	$-2.16(9)\times10^{-3}$
1/4	1.6195	0.539 64(2)	0.159 01(2)	$1.9622(9)\times10^{-2}$	$-1.16(5)\times10^{-3}$	$-2.4(2)\times10^{-4}$
4	1.6195	0.483 82(2)	0.112 45(2)	$2.075(9)\times10^{-2}$	$8.88(4)\times10^{-3}$	$2.9(5)\times10^{-4}$
1/3	1.3634	0.562 83(2)	0.194 08(2)	$4.352(3)\times10^{-2}$	$8.03(5)\times10^{-3}$	$2.12(5)\times10^{-3}$
3	1.3634	0.532 41(2)	0.166 48(2)	$4.035(3)\times10^{-2}$	$1.243(5)\times10^{-2}$	$3.17(8)\times10^{-3}$
1/2.75	1.3027	0.570 11(2)	0.205 00(2)	$5.120(9)\times10^{-2}$	$1.128(3)\times10^{-2}$	$3.107(5)\times10^{-3}$
2.75	1.3027	0.545 70(2)	0.182 47(2)	$4.761(8)\times10^{-2}$	$1.437(4)\times10^{-2}$	$3.95(4)\times10^{-3}$
1/1.25	1.0133	0.621 40(2)	0.281 74(3)	0.106 43(3)	$3.706(4)\times10^{-2}$	$1.225(4)\times10^{-2}$
1.25	1.0133	0.621 11(2)	0.281 43(3)	0.106 34(9)	$3.696(4)\times10^{-2}$	$1.219(3)\times10^{-2}$

gence properties. We then use our data to calculate the coefficients in the y expansion[29,30] and investigate how well the y expansion fares in reproducing simulation data. Finally, we present a brief analysis of the radius of convergence of the virial series based on a Padé analysis and finish off with a few words of conclusion.

II. CALCULATIONS AND RESULTS

The virial coefficients B_n with $n=2,3,\ldots$ are the expansion coefficients of the compressibility factor $Z=p/kT\rho$ (p, T, and k are the pressure, temperature, and Boltzmann constant, respectively) in powers of the number density ρ,

$$Z = 1 + \sum_{n\geqslant 2} B_n \rho^{n-1}. \tag{1}$$

The virial coefficients B_n depend on the interparticle interactions and may be written in the form

$$B_n = \frac{1-n}{n!} \int \cdots \int V_n \prod_{j=1}^{n} d\mathbf{r}_j. \tag{2}$$

Extremely useful expressions for V_n were provided by Ree and Hoover[6,7] and they developed a Monte Carlo (MC) procedure which allowed them to calculate the first seven virial coefficients for hard discs and hard spheres. The eighth virial was later calculated by van Rensburg using a similar scheme.[8,9] Vlasov *et al.*[10] recently improved the algorithm by taking into account all possible topologically equivalent graphs that contribute to V_8. This is related to the unlabeling factors discussed by Ree and Hoover[6,7] and results in a more efficient method. Very recently B_9 and B_{10} have been calculated for hard hyperspheres.[11,12]

The MC method is not, however, restricted simply to hard spheres and discs. Given an overlap test that can determine whether two particles do or do not overlap, the method can be used to determine the virial coefficients for any hard body. Sample results were given previously.[10] We now proceed to give a fuller discussion.

A crucial ingredient for carrying out the MC integrations to obtain the virial coefficients is an efficient overlap test. The overlap test used for spheroids is that devised by Perram and Wertheim,[31] while the overlap tests for spherocylinders and truncated spheres are given in Ref. 32. In order to create the necessary spanning trees of overlapping particles, one must be careful not to introduce any bias in how one generates the overlaps. In this work we used the simplest placement scheme, i.e., a particle was placed in a random position within a box centered on the target particle and the orientation was also chosen completely at random. The dimensions of the box were chosen to be sufficiently big that no overlap would be possible should the particle be placed outside the box. The placement is repeated until an overlap results, and this establishes the particular link in the spanning tree. It is possible to come up with more efficient placement schemes (i.e., that produces a higher fraction of successful overlaps), but our experience was that the increased computational labor of implementing such schemes often outweighed the benefits obtained by the higher success rate. Also one could, all too easily, introduce an accidental bias that would lead to inaccurate results.

To estimate B_3 through to B_7 10^9 random configurations were used. The errors were estimated using the method described by Ree and Hoover.[6,7] Our methodology gave identical answers for the lower-order virials to those published earlier, which serves as a check on our overlap and random placement routines.

The quantity directly calculated is the virial coefficient normalized by an appropriate power of B_2, i.e., one calculates $\tilde{B}_n = B_n/B_2^{n-1}$. Our results for spheroids are given in Table I, our results for spherocylinders are in Table II, and the truncated sphere results are in Table III. For completeness, we quote our values for the first seven virial coefficients, also giving the values of the second virials, which are simple analytic expressions for spherocylinders and truncated spheres and which may be calculated as accurately as one wishes for hard spheroids.[16]

For spheroids we denote the semimajor axis by a and the semiminor axis by b. The aspect ratio is given by a/b. For $a/b>1$, the spheroid is prolate, while for $a/b<1$ the spheroid is oblate. In Table I we present our data on B_2-B_7 for

TABLE II. The reduced virial coefficients ($\tilde{B}_3$ to $\tilde{B}_7$) for hard spherocylinders (length L and diameter D) and the second virial B_2 in terms of the spherocylinder volume v_0. The estimated error is the final figure given in parentheses.

L/D	B_2/v_0	$\tilde{B}_3$	$\tilde{B}_4$	$\tilde{B}_5$	$\tilde{B}_6$	$\tilde{B}_7$
3.0	18.588	0.489 78(2)	0.118 16(2)	$2.159(3)\times10^{-2}$	$8.74(4)\times10^{-3}$	$9.5(6)\times10^{-4}$
3.2	20.190	0.481 64(2)	0.109 77(2)	$1.935(3)\times10^{-2}$	$8.510(4)\times10^{-3}$	$5.3(6)\times10^{-4}$
4.0	27.227	0.451 62(2)	$8.085(2)\times10^{-2}$	$1.359(3)\times10^{-2}$	$7.97(4)\times10^{-3}$	$-1.41(6)\times10^{-3}$
5.0	37.437	0.419 40(2)	$5.271(2)\times10^{-2}$	$1.110(3)\times10^{-2}$	$7.34(4)\times10^{-3}$	$-3.69(6)\times10^{-3}$
10.0	112.050	0.312 57(2)	$-1.618(2)\times10^{-2}$	$2.259(3)\times10^{-2}$	$-3.95(4)\times10^{-3}$	$-5.51(7)\times10^{-3}$

aspect ratios ranging from 0.1 to 10, i.e., from thin discs to long rods. Our results for the lower-order virials are in agreement with previous works.[13,16–18] For the more spherical particles ($1/3 \leqslant a/b \leqslant 3$) all seven virials are positive, as is the case for hard spheres. For less spherical particles, negative virials appear. This has been noted before for the lower-order virials.[13,17,18] Thus for oblate spheroids, B_6 is negative for $a/b \leqslant 1/4$. B_7 is negative for $a/b \leqslant 1/4$ and $a/b \geqslant 5$.

The equation of state for prolate spheroids (aspect ratio a/b) is approximately the same as that for oblate spheroids with the inverse aspect ratio (i.e., b/a).[16,33] The second virial coefficients of these spheroids are equal,[16] but no such symmetry holds for the higher virial coefficients. For hard spheroids with moderate anisotropy (e.g., $1/3 \leqslant a/b \leqslant 3$) the prolate and oblate virial coefficients (B_3 to B_7) are rather similar and this leads to the approximate similarities in the equation of state. When the spheroids are more anisotropic, the coefficients differ significantly and it would appear to be fortuitous that the equations of state are so similar. Similar conclusions were reached by Vega and Lago[18] on the basis of the knowledge of five virial coefficients.

For spherocylinders, we denote the length of the cylinder by L and the diameter of the cylinder by D. In Table II, we present results for L/D ranging from 3 to 10. Again the values of the lower-order virials agree with previous results.[13,19,20] Negative virials once more make an appearance. B_6 is negative for $L/D=10$ and we find negative values for B_7 for $L/D \geqslant 4$.

For truncated spheres, we present in Table III our results for aspect ratios ranging from infinitely thin discs ($L/D=0$) to hard spheres ($L/D=1$). Here we denote the thickness of the disc by L and the diameter of the sphere by D. Again our results for the lower-order virials agree with previous calculations.[20] B_6 and B_7 are negative for $L/D \leqslant 0.2$. It is worth noting that for spherocylinders, $\tilde{B}_6$ and $\tilde{B}_7$ both decrease as L/D increases. For truncated spheres, the $\tilde{B}_6$ virial coefficient is negative for infinitely thin hard discs, but as the thickness increases, $\tilde{B}_6$ also increases, becoming positive for $L/D > 0.3$. $\tilde{B}_7$ is positive for infinitely thin discs and, with increasing thickness, decreases to a minimum before increasing again.

III. DISCUSSION

A. Virial equation of state

We now turn to the question as to how well the virial series can predict the equation of state. In all cases we show the variation of the reduced pressure, $p^*=p v_0/kT$, with volume fraction, $\eta=v_0\rho$. Here v_0 is the volume of the hard particle. To avoid overburdening the reader with graphs, we choose just one or two examples of typical behavior for each type of particle. We also reiterate that the virial expansion considered here applies only to the isotropic phase. The simulation data sometimes refer to both isotropic and liquid-crystalline phases, so in the text we will indicate the packing fraction at which the isotropic phase is no longer stable.

We first consider hard spheroids. The equation of state for spheroids of aspect ratio 3 and 10 are plotted in Figs. 1 and 2, respectively. We compare simulation results[23,33,34]

TABLE III. The reduced virial coefficients ($\tilde{B}_3$ to $\tilde{B}_7$) for hard truncated spheres (thickness L and diameter D) and the second virial B_2 in units of D^3. The estimated error is the final figure given in parentheses.

L/D	B_2/D^3	$\tilde{B}_3$	$\tilde{B}_4$	$\tilde{B}_5$	$\tilde{B}_6$	$\tilde{B}_7$
0.0	0.616 85	0.444 64(2)	$1.993(2)\times10^{-2}$	$-6.0339(3)\times10^{-2}$	$-1.730(5)\times10^{-2}$	$1.57(7)\times10^{-3}$
0.05	0.736 95	0.479 93(2)	$7.114(2)\times10^{-2}$	$-3.334(3)\times10^{-2}$	$-1.470(5)\times10^{-2}$	$-5.6(7)\times10^{-4}$
0.1	0.855 54	0.508 05(2)	0.111 83(2)	$-1.031(3)\times10^{-2}$	$-1.039(4)\times10^{-2}$	$-1.40(6)\times10^{-3}$
0.15	0.971 86	0.520 52(2)	0.144 43(2)	$9.12(3)\times10^{-3}$	$-5.49(4)\times10^{-3}$	$-1.27(6)\times10^{-3}$
0.2	1.085 21	0.548 58(2)	0.170 91(2)	$2.561(3)\times10^{-2}$	$-4.3(4)\times10^{-4}$	$-8.4(6)\times10^{-4}$
0.3	1.300 52	0.575 09(2)	0.209 72(2)	$5.101(3)\times10^{-2}$	$8.72(4)\times10^{-3}$	$1.10(5)\times10^{-3}$
0.4	1.496 90	0.605 33(2)	0.255 04(3)	$8.334(3)\times10^{-2}$	$1.644(4)\times10^{-2}$	$3.13(5)\times10^{-3}$
0.5	1.670 44	0.605 33(2)	0.255 04(2)	$8.334(3)\times10^{-2}$	$2.297(3)\times10^{-2}$	$5.51(5)\times10^{-3}$
0.6	1.817 80	0.613 95(2)	0.268 46(3)	$9.398(3)\times10^{-2}$	$2.869(3)\times10^{-2}$	$7.75(5)\times10^{-3}$
0.7	1.936 11	0.619 74(2)	0.277 91(3)	0.101 96(3)	$3.343(3)\times10^{-2}$	$1.008(5)\times10^{-2}$
0.8	2.022 96	0.623 24(2)	0.283 79(3)	0.107 30(3)	$3.682(3)\times10^{-2}$	$1.187(4)\times10^{-2}$
0.9	2.076 29	0.624 77(2)	0.286 52(2)	0.109 82(3)	$3.852(3)\times10^{-2}$	$1.288(4)\times10^{-2}$
1.0	2.094 40	0.625	0.2869	0.110 252(1)	$3.881(6)\times10^{-2}$	$1.305(2)\times10^{-2}$

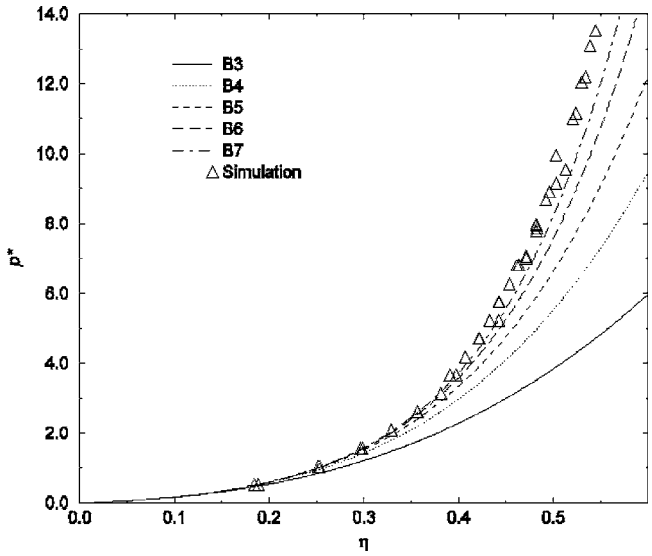

FIG. 1. The virial equation of state for prolate spheroids with $a/b=3$ for various levels of truncation, as indicated in the legend. The triangles are simulation data (Ref. 31).

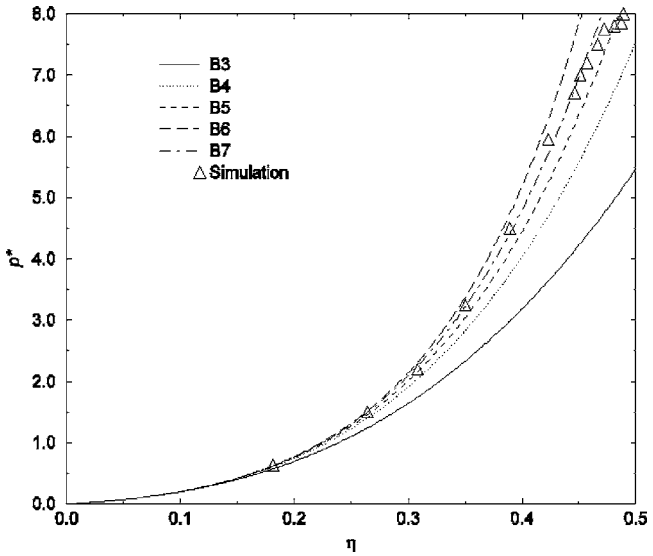

FIG. 3. The virial equation of state of spherocylinders with $L/D=4$ for various levels of truncation, as indicated in the legend. The triangles are simulation data (Ref. 33).

with the predictions of the virial expansion [Eq. (1)] and, to help assess the rate of convergence of the series, we plot the predictions for various levels of truncation of the series.

Figure 1 is for prolate spheroids of moderate anisotropy ($a/b=3$). It would appear that the more virial coefficients we use, the closer is the agreement with simulation data[33]—the same as is found for hard spheres. Indeed when we include our current estimate of B_8, the virial predictions are yet more accurate. The packing fraction of the isotropic phase at the isotropic-nematic transition is 0.56.[33]

For highly anisotropic particles, however, the virial expansion is considerably less well-behaved. Figure 2, for prolate spheroids with $a/b=10$, shows typical behavior. Except for rather low densities, the virial expansion does not seem to be convergent. Indeed for certain levels of truncation of the series, one finds that increasing the density leads to a decrease of pressure, with the pressure becoming negative at sufficiently high densities. From simulation the isotropic phase is stable up to a packing fraction of 0.22.[23,34]

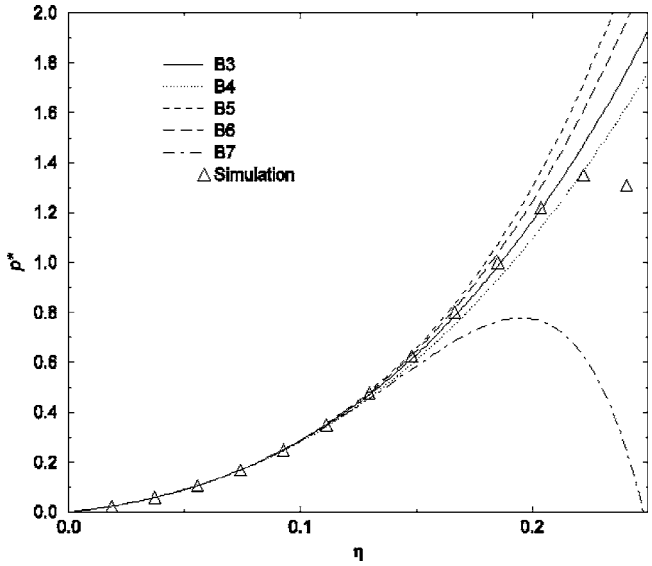

FIG. 2. The virial equation of state of prolate spheroids with $a/b=10$ for various levels of truncation, as indicated in the legend. The triangles are simulation data (Ref. 32).

We now turn to hard spherocylinders. In Fig. 3 we compare the virial EOS with simulation[35] for spherocylinders with an aspect ratio $L/D=4$. Here the virial expansion seems to be approaching the simulation results as one adds more and more virials. The simulation studies indicate that the isotropic phase is stable up to a packing fraction of 0.47. For more anisotropic particles, however, one regains plots resembling those for highly anisotropic spheroids—convergence is limited to a small density range.

Finally, we consider truncated hard spheres. In Fig. 4 we compare the virial predictions with simulation data[20] for thin truncated spheres with $L/D=0.1$. Again the convergence properties are poor and negative pressures are found at high densities for certain levels of truncation of the virial series. In this case the isotropic phase is stable up to $\eta=0.30$.[20]

In summary it seems that all seven virial coefficients are positive for particles with small anisotropies, and the virial series appears to converge over a wide range of densities. For greater anisotropies, however, negative virial coefficients appear and these seem to have a damaging effect on convergence. The general rule is that the more anisotropic the particle, the smaller is the range of volume fraction for which the series is convergent. Clearly some form of resummation of the series is needed in these cases and we now turn to the y expansion proposed by Barboy and Gelbart.[29,30]

B. The *y* expansion

Barboy and Gelbart observed that for a number of hard-core fluids, an n-term y expansion tends to reproduce the true equation of state better than the corresponding n-term virial series. This expansion takes the form

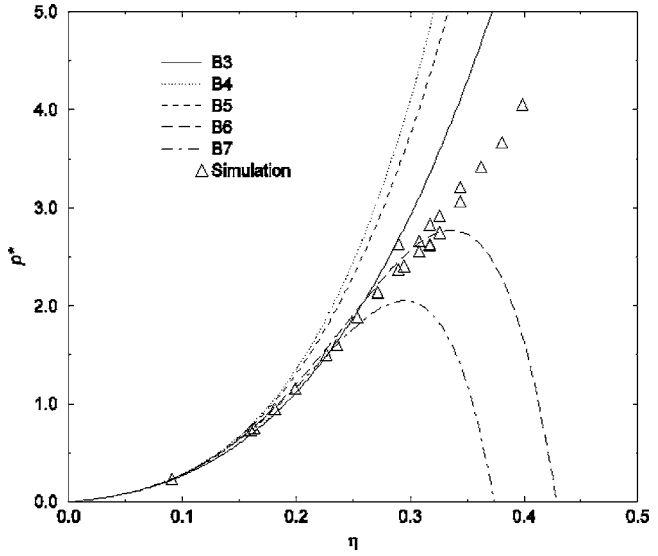

FIG. 4. The virial equation of state of truncated spheres with $L/D=0.1$ for various levels of truncation, as indicated in the legend. The triangles are simulation data (Ref. 20).

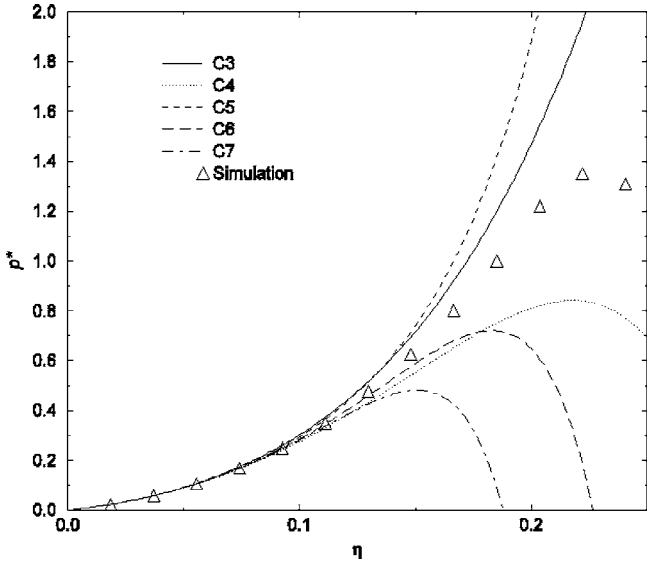

FIG. 6. The equation of state for prolate spheroids with $a/b=10$ for various levels of truncation of the y expansion, as indicated in the legend. The triangles are simulation data (Ref. 32).

$$p^* = \sum_{n=1} C_n y^{n-1}, \tag{3}$$

where $y=\eta/(1-\eta)$. The coefficient C_n is given in terms of the virial coefficients of order less than or equal to n.

We calculated the coefficients of the y expansion for the cases discussed previously, i.e., spheroids with $a/b=3$ and 10, spherocylinders with $L/D=4$, and truncated spheres with $L/D=0.1$. We compare the predictions of the y expansion, truncated at various levels, with simulation data in Figs. 5–8.

In the less anisotropic cases, such as spheroids with $a/b=3$, the y expansion does initially converge faster than the virial series. Indeed a third-order expansion is in very reasonable agreement with simulation, see Fig. 5. However, as one goes to higher order, the y expansion is arguably less well-behaved than the virial expansion—note the bad behavior on truncating at the C_7 term. For more anisotropic particles (e.g., spheroids with $a/b=10$), where the virial series converged badly, the y expansion fares no better. As Fig. 6 shows, we once again find that negative pressures may be predicted at high densities and adding more terms to the series does not improve agreement with simulation. Similar conclusions hold for spherocylinders and truncated spheres (Figs. 7 and 8).

In conclusion, we believe that a low-order y expansion is superior to an equivalently low-order virial expansion for near-spherical models, but at higher order, there is little to choose between the two expansions. Indeed there is some evidence that the virial expansion is superior at high order. For more anisotropic particles both expansions are equally poorly convergent.

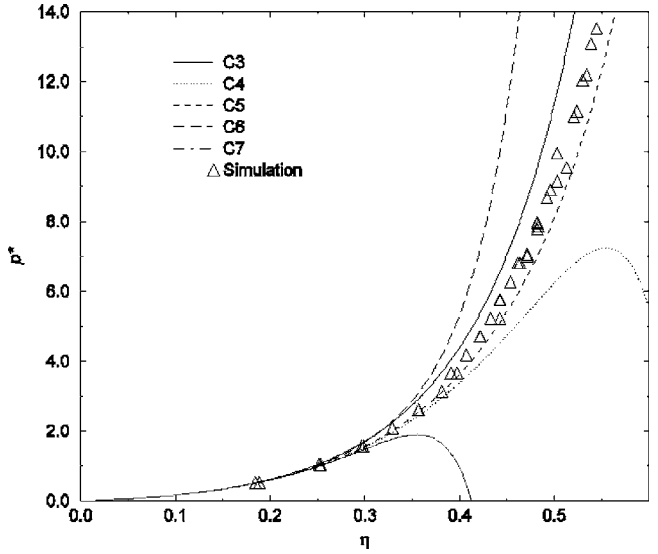

FIG. 5. The equation of state for prolate spheroids, $a/b=3$, for various levels of truncation of the y expansion, as indicated in the legend. The triangles are simulation data (Ref. 31).

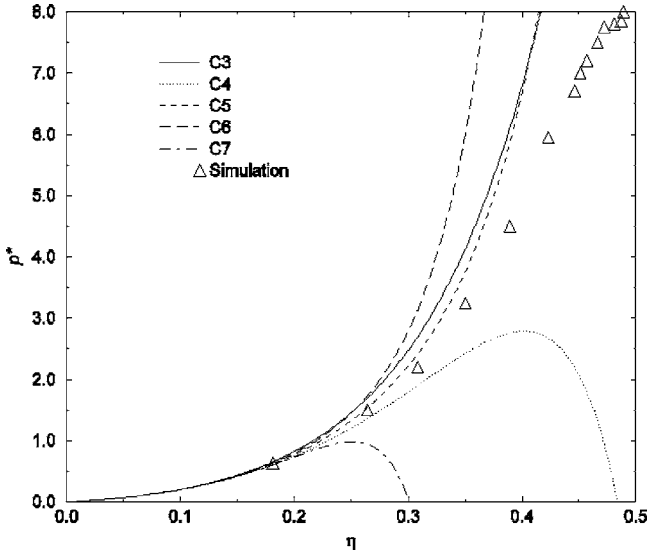

FIG. 7. The equation of state of spherocylinders with $L/D=4$ for various levels of truncation of the y expansion, as indicated in the legend. The triangles are simulation data (Ref. 33).

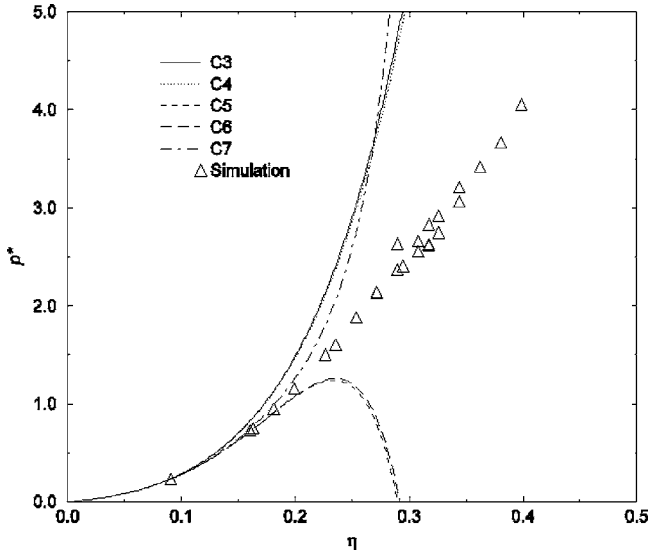

FIG. 8. The equation of state of truncated spheres with $L/D=0.1$ for various levels of truncation of the y expansion, as indicated in the legend. The triangles are simulation data (Ref. 20).

C. Padé analysis

In order to estimate the radius of convergence of the virial series, we use a Padé analysis. The $[n/m]$ Padé approximant for the compressibility factor Z is denoted by $Z_{n,m}$ and is given by

$$Z_{n,m}=\frac{1+\sum_{i=1}^{n}a_i\eta^i}{1+\sum_{i=1}^{m}b_i\eta^i}.$$

The coefficients, a_i and b_i, are chosen so that a virial expansion of the approximant gives the correct values of the first $n+m$ virial coefficients. We may estimate the radius of convergence of the virial series by finding the root of the denominator with the smallest modulus. There are, however, certain caveats in this procedure that we should note. Firstly, these estimates will vary with the values chosen for m and n, but we know that we should only trust fairly symmetrical approximants (i.e., when m and n are not too different). We have examined as many possibilities as we can, given the limited number of virial coefficients available, but here we only present results for $Z_{3,3}$—the symmetrical approximant that makes use of all seven virial coefficients. The general conclusions that follow are not qualitatively changed either by looking at lower-order approximants or by including our current estimates of B_8 to obtain higher-order approximants. Secondly, we need to check that the numerator and denominator do not have very similar zeros. In this case the approximant is termed defective and is not trustworthy. Here we class an approximant as defective if the zeros differ by less than 1%. Finally, we note that statistical errors in the virial coefficients can sometimes have a marked effect on the calculated roots. We have estimated the errors in our calculated zeros by repeating the calculations, varying the virial coefficients by a standard mean error, and seeing how the results change.

TABLE IV. The poles of the Padé $Z_{3,3}$ approximant for hard spheroids (semimajor axis a and semiminor axis b). The estimated error is the final figure given in parentheses. When it exists, η_+ is the smallest real, positive pole. For significantly anisotropic particles, η is the pole of smallest modulus and we have attempted to track its behavior as the particles become more spherical. A complex pole is denoted by an asterisk, while a dash indicates a defective approximant. η_{IN} is the packing fraction of the isotropic phase at the isotropic-nematic transition, as obtained from simulation studies.

a/b	η_+	η	η_{IN}
10	—	—	0.22[a]
7	—	—	
5	0.606(2)	−0.207(7)	0.35[a]
4	0.635(1)	−0.33(1)	
3	0.662(4)	−0.9(2)	0.51[b]
2.75	0.673(2)	−1.057(1)	0.56[b]
1/2.75	0.66(1)	0.82(2)*	0.54[b]
1/3	0.66(1)	0.76(2)*	0.5[b]
1/4	0.737(7)	0.607(3)*	
1/5	0.810(3)	0.472(7)*	0.31[a]
1/7		0.3559(4)*	
1/10		0.2365(1)*	0.19[a]

[a]Reference 32.
[b]Reference 31.

In Table IV, the second column gives the smallest positive, real pole of the $Z_{3,3}$ approximant. For significantly anisotropic particles, the pole with the smallest modulus is either real and negative or it is complex. In the third column we give this pole for the highly anisotropic cases and we attempt to track its behavior as the particles become more and more spherical. For sufficiently spherical particles, the real positive pole has the smallest modulus.

The general conclusions are as follows: Firstly, as expected, the radius of convergence decreases as the particle becomes more anisotropic. For fairly spherical particles, the pole of smallest modulus is real and positive and its value is reasonably close to the packing fraction of closest crystalline packing (0.7048). Indeed if one constructs a higher-order approximant based on our present, tentative estimates of B_8, the pole gets closer to the close-packing value. As the particles become less spherical, the pole of lowest modulus is either real and negative (prolate) or is complex (oblate) and it is this pole that determines the radius of convergence of the series. For $1/5 \leqslant a/b \leqslant 5$ there exists a positive real pole, with a modulus close to the density at closest packing, but this pole only controls the radius of convergence of the series for $1/3 \leqslant a/b \leqslant 3$.

Naturally one requires many more virial coefficients to firm up this analysis, but the general observation that for highly aspherical hard particles the radius of convergence is much less than the density of closest packing is also very clear just from a casual study of Figs. 2 and 4.

Assuming the Padé analysis is at least qualitatively valid, one may ask if the negative or complex poles governing the radius of convergence have any physical interpretation. Two possibilities that spring to mind are either a density related to the isotropic-nematic transition or else a maximum random-packing density with the constraint that the orienta-

tions are isotropically distributed. It is, however, difficult to explain on this basis why the relevant root is not real and positive and, indeed, there are no obvious physical arguments to support either of these hypotheses.

While the radius of convergence of the virial expansion for significantly aspherical particles would appear to be much less than the packing fraction at close packing, an important question is whether the series is convergent for packing fractions up to the isotropic-nematic transition, should it occur. These values are also listed in Table IV. A comparison of these values with the estimates of the radius of convergence of the isotropic virial series suggests that the virial series may provide a good account of the isotropic equation of state up to the isotropic-nematic transition density.

IV. CONCLUSIONS

We have calculated the sixth and seventh virial coefficients for a variety of hard bodies. We have presented results for hard spheroids with aspect ratios ranging from 1/10 (oblate) to 10 (prolate), for hard spherocylinders with L/D ranging from 3 to 10, and for hard truncated spheres with L/D ranging from 0 (infinitely thin discs) to 1 (hard spheres).

We then examined the predicted equations of state and compared these, where possible, with computer simulation data. Our conclusion is that for reasonably spherical particles, the more virial coefficients one includes, the closer one approaches the simulation results. For longer or flatter particles, however, negative virials start to make an appearance and these seriously affect the convergence properties of the series. Indeed the range of packing fractions for which the series converges seems to decrease with increasing asphericity.

We also investigated the convergence properties of the y expansion. For fairly spherical particles, a low-order y expansion is more accurate than a correspondingly low-order virial expansion, but at higher order the virial expansion is arguably superior. For more anisotropic particles, the convergence of the y expansion is no better than that of the virial expansion.

Finally, we used a Padé analysis to investigate the radius of convergence of the virial series. The indications are that for fairly spherical particles, the radius of convergence is determined by a real, positive pole, whose value is in the vicinity of the density of closest packing. As the particle becomes less spherical a second pole, either negative or complex, has the smallest modulus and this determines the radius of convergence of the series.

In reality, of course, highly aspherical particles may form a nematic crystalline phase at low packing fractions. This is certainly the case for the axially symmetric particles considered here. Thus if one wished to use the virial series to calculate the phase diagram for these particles, a relevant question is whether or not the virial expansion for the isotropic phase converges for densities up to the isotropic-nematic transition density. Looking at our estimates of the radius of convergence and also at simulation values for the isotropic-nematic transition densities, it would appear that the values are fairly similar (though we do not wish to claim any exact correspondence). It is thus quite possible that the virial series approach will prove useful in predicting the liquid-crystalline-phase behavior and we shall study this in detail in a series of future papers.

ACKNOWLEDGMENTS

We gratefully acknowledge the support of Universities UK in providing an Overseas Research Studentship (ORS) award to one of the authors (X.Y.) and a grant from the Engineering and Physical Sciences Research Council (EPSRC) for funding one of the authors (A.Yu.V.). We are also grateful to Mike Allen for providing us with overlap routines for spheroids and spherocylinders and to R. Blaak for use of his cut-sphere overlap routine. We also thank Mike Allen and George Jackson for providing us with equation-of-state data for spheroids and spherocylinders, respectively.

[1] D. A. McQuarrie, *Statistical Mechanics* (Harper and Row, New York, 1976).
[2] E. A. Mason and T. H. Spurling, *The Virial Equation of State*, in The International Encyclopedia of Physical Chemistry and Chemical Physics Vol. 2 (Pergamon, Oxford, 1969).
[3] J.-P. Hansen and I. R. McDonald, *Theory of Simple Liquids* (Academic, London, 1986).
[4] J. L. Lebowitz and O. Penrose, J. Math. Phys. **5**, 841 (1964).
[5] I. P. Bazarov and P. N. Nikolaev, Dokl. Akad. Nauk SSSR **296**, 321 (1987).
[6] F. H. Ree and W. G. Hoover, J. Chem. Phys. **40**, 939 (1964).
[7] F. H. Ree and W. G. Hoover, J. Chem. Phys. **46**, 4181 (1967).
[8] E. J. J. van Rensburg and G. M. Torrie, J. Phys. A **26**, 943 (1992).
[9] E. J. J. van Rensburg, J. Phys. A **26**, 4805 (1993).
[10] A. Yu. Vlasov, X. M. You, and A. J. Masters, Mol. Phys. **100**, 3313 (2002).
[11] N. Clisby and B. M. McCoy, J. Stat. Phys. **114**, 1361 (2004).
[12] N. Clisby and B. M. McCoy, cond-mat/0410511.
[13] T. Boublik and I. Nezbeda, Collect. Czech. Chem. Commun. **51**, 2301 (1986).
[14] A. Baram and M. Luban, J. Phys. C **12**, L659 (1979).
[15] I. C. Sanchez, J. Chem. Phys. **101**, 7003 (1994).
[16] B. Mulder and D. Frenkel, Mol. Phys. **55**, 1193 (1985).
[17] M. Rigby, Mol. Phys. **66**, 1261 (1989).
[18] C. Vega and S. Lago, J. Chem. Phys. **56**, 6727 (1994).
[19] D. Frenkel, J. Phys. Chem. **91**, 4915 (1987); **92**, 5314 (1989).
[20] E. Velasco and P. Padilla, Mol. Phys. **94**, 335 (1998).
[21] J. A. C. Veerman and D. Frenkel, Phys. Rev. A **45**, 5633 (1992).
[22] J. D. Parsons, Phys. Rev. A **19**, 1225 (1979).
[23] S.-D. Lee, J. Chem. Phys. **87**, 4972 (1987).
[24] S.-D. Lee, J. Chem. Phys. **89**, 7036 (1989).
[25] For a recent example, see, e.g., S. Varga, A. Galindo, and G. Jackson, Mol. Phys. **101**, 817 (2003).
[26] B. Tjipto-Margo and G. T. Evans, J. Chem. Phys. **93**, 4254 (1990).
[27] A. Samborski, G. T. Evans, C. P. Mason, and M. P. Allen, Mol. Phys. **81**, 263 (1994).
[28] P. J. Camp, M. P. Allen, and A. J. Masters, J. Chem. Phys. **111**, 9871 (1999).
[29] B. Barboy and W. M. Gelbart, J. Chem. Phys. **71**, 3053 (1979).
[30] B. Barboy and W. M. Gelbart, J. Stat. Phys. **22**, 709 (1980).
[31] J. W. Perram and M. S. Wertheim, J. Comput. Phys. **58**, 409 (1985).
[32] M. P. Allen, G. T. Evans, D. Frenkel, and B. M. Mulder, Adv. Chem. Phys. **86**, 1 (1993).
[33] D. Frenkel and B. Mulder, Mol. Phys. **55**, 1171 (1985).
[34] P. J. Camp, C. P. Mason, M. P. Allen, A. A. Khare, and D. A. Kofke, J. Chem. Phys. **105**, 2837 (1996).
[35] S. C. McGrother, D. C. Williamson, and G. Jackson, J. Chem. Phys. **104**, 6755 (1996).